CMI

www.nature.com/cmi

ARTICLE

Check for updates

# CD200R$^{high}$ neutrophils with dysfunctional autophagy establish systemic immunosuppression by increasing regulatory T cells

Ye Seon Kim[1], Yu Sun Jeong[1], Geon Ho Bae[1,4], Ji Hyeon Kang[1], Mingyu Lee[2], Brian A. Zabel[3] and Yoe-Sik Bae[1,2]✉



Distinct neutrophil populations arise during certain pathological conditions. The generation of dysfunctional neutrophils during sepsis and their contribution to septicemia-related systemic immune suppression remain unclear. In this study, using an experimental sepsis model that features immunosuppression, we identified a novel population of pathogenic CD200R$^{high}$ neutrophils that are generated during the initial stages of sepsis and contribute to systemic immune suppression by enhancing regulatory T ($T_{reg}$) cells. Compared to their CD200R$^{low}$ counterparts, sepsis-generated CD200R$^{high}$ neutrophils exhibit impaired autophagy and dysfunction, with reduced chemotactic migration, superoxide anion production, and TNF-α production. Increased soluble CD200 blocks autophagy and neutrophil maturation in the bone marrow during experimental sepsis, and recombinant CD200 treatment in vitro can induce neutrophil dysfunction similar to that observed in CD200R$^{high}$ neutrophils. The administration of an α-CD200R antibody effectively reversed neutrophil dysfunction by enhancing autophagy and protecting against a secondary infection challenge, leading to increased survival. Transcriptome analysis revealed that CD200R$^{high}$ neutrophils expressed high levels of *Igf1*, which elicits the generation of $T_{reg}$ cells, while the administration of an α-CD200R antibody inhibited $T_{reg}$ cell generation in a secondary infection model. Taken together, our findings revealed a novel CD200R$^{high}$ neutrophil population that mediates the pathogenesis of sepsis-induced systemic immunosuppression by generating $T_{reg}$ cells.

**Keywords:** Sepsis; Neutrophils; CD200R; Autophagy; IGF-1; Regulatory T cells

*Cellular & Molecular Immunology* (2024) 21:349–361; https://doi.org/10.1038/s41423-024-01136-y

## INTRODUCTION

Sepsis, a serious systemic inflammatory syndrome caused by infection, is a life-threatening disease [1]. To date, many different therapeutic approaches have been implemented to improve outcomes in septic patients by targeting pathogen-associated molecules, inflammatory mediators, and regulators of coagulation [2, 3]. Unfortunately, all of those approaches have failed, showing no significant therapeutic effects [4, 5]. An important reason for these clinical failures may be that the experimental animal models used in preclinical studies are focused mainly on the excessively immune-activated stage and do not recapitulate human clinical sepsis with respect to immune suppression [6]. In the clinic, sepsis patients are treated with antibiotics (ABX) to control bacterial infection [7, 8]. Patients who survive initial septicemia may develop profound immunosuppression, characterized by diminished and dysfunctional leukocytes and succumb to secondary infections [9]. It is known that neutrophils are dysfunctional under septic conditions [9–11]. Neutrophil dysfunction is a pivotal trait associated with sepsis-induced immunosuppression. This dysfunction significantly elevates vulnerability to secondary infections, especially given that neutrophils play a critical role in host defense against the majority of the clinically relevant pathogens affecting hospitalized patients, such as *Pseudomonas aeruginosa*, *Staphylococcus aureus* (*S. aureus*), and *Candida albicans*. The increase in dysfunctional neutrophils during septic conditions is closely linked to the heightened production of immature neutrophils through a process known as 'emergency granulopoiesis' [12]. Emergency granulopoiesis is the swift generation of neutrophils in response to elevated demands, such as infections. This process is characterized by a surge in the release of immature neutrophils into the bloodstream. Because neutrophils play essential roles in the innate immune defense against invading bacteria [13], understanding the mechanisms and nature of neutrophil dysfunction during sepsis is critical. However, specific immunophenotypic markers for dysfunctional neutrophils have yet to be identified.

Immune checkpoint receptors and their ligands are involved in the regulation of immune activation in infectious or inflammatory disorders, as well as cancer [14]. Elevated expression levels of immune checkpoint proteins, such as CTLA4, PD-1, and PD-L1, are prominent hallmarks of immunosuppressive states in both cancer and sepsis [15, 16]. These immune checkpoint proteins, including CTLA4, PD-1, PD-L1, LAG3, and TIM3, are well characterized and found on a range of cell types, including T cells, antigen-presenting cells, and tumor cells [17, 18]. The functional roles of checkpoint receptor-checkpoint ligand interactions have been

[1]Department of Biological Sciences, Sungkyunkwan University, Suwon 16419, Republic of Korea. [2]Department of Health Science and Technology, SAIHST, Sungkyunkwan University, Seoul 06351, Republic of Korea. [3]Palo Alto Veterans Institute for Research, Veterans Affairs Hospital, Palo Alto, CA 94304, USA. [4]Present address: Division of Immunology, Boston Children's Hospital, Boston, MA, USA. ✉email: yoesik@skku.edu

Received: 24 April 2023 Revised: 21 December 2023 Accepted: 13 January 2024
Published online: 5 February 2024

extensively studied in cancer [15]. Recently, it has been reported that the expression of these checkpoint receptors and their ligands is also upregulated in lymphocytes and monocytes during sepsis [19]. However, whether immune checkpoint proteins regulate neutrophil activity under septic conditions has not been determined.

In our study, we established an immunosuppressive model using cecal ligation and puncture (CLP) combined with ABX treatment (referred to as CLP + ABX) to simulate clinical conditions. With this animal model, we identified a previously unrecognized subset of neutrophils that exhibited upregulated expression of CD200R, a checkpoint receptor, and showed signs of functional impairment. Notably, the CD200 level was found to increase during sepsis, and this change hindered G-CSF-induced autophagy, a crucial process for neutrophil maturation and functionality. Administration of an α-CD200R antibody successfully restored neutrophil maturity and autophagic activity. These alterations in neutrophils significantly impact their ability to combat secondary infections, a critical complication associated with sepsis-induced immunosuppression. Furthermore, the upregulated CD200R expression on neutrophils leads to systemic immunosuppression by triggering the production of insulin-like growth factor 1 (IGF-1), resulting in the induction of regulatory T ($T_{reg}$) cells. Our findings highlight the importance of CD200R as a key regulator in neutrophils that drives sepsis-induced immunosuppression, offering novel insights into the biology of CD200R and dysfunctional neutrophils.

## RESULTS

### CD200R-expressing immature neutrophils are generated after the establishment of an experimental sepsis-induced immunosuppressive model

Sepsis-induced immunosuppressive model mice were constructed by performing CLP surgery followed by ABX administration (Fig. 1A). Mice were sacrificed 72 h after surgery, and neutrophil differentiation was assessed by analyzing the levels of c-kit and Ly6G following the gating strategy outlined in a previous report [20] (Fig. 1 and Fig. S1). CLP + ABX significantly increased myelocyte (MC), metamyelocyte (MM) and band cell (BC) counts but decreased the number of mature neutrophils (polymorphonuclear neutrophils, PMNs) compared to those in sham-operated mice, as determined by Ly6G and c-kit staining (Fig. 1B and Fig. S2). Mice in the sham group, which were injected with ABX alone without CLP surgery, exhibited no alterations in neutrophil differentiation (Fig. S2). Giemsa staining confirmed that the number of segmented mature neutrophils was significantly reduced (Fig. 1C). The frequency of the mature neutrophil marker CD101 was significantly lower in neutrophils from CLP + ABX animals than in those from sham animals, as determined by flow cytometry (Fig. 1D). CXCR2 expression is important for mature neutrophil egress from the bone marrow to the peripheral blood [21], while CXCR4 is important for the retention of immature neutrophils in the bone marrow [22]. Compared with those from sham mice, neutrophils from CLP + ABX mice had significantly downregulated CXCR2 expression but upregulated CXCR4 expression (Fig. 1E), collectively suggesting an increase in immature neutrophils in the sepsis-induced immunosuppressive model.

The expression of coinhibitory molecules is closely associated with immune suppression in several types of leukocytes, including T lymphocytes [23]. Here, we compared the expression patterns of coinhibitory molecules on neutrophils isolated from control or CLP + ABX mice. The surface expression levels of PD-1, PD-L1, and CD200R on neutrophils from CLP + ABX mice were greater than those on neutrophils from control mice (Fig. 1F). There were very few $CD101^+$ mature neutrophils in the CLP + ABX mice (Fig. 1D). Furthermore, when comparing $CD101^-$ immature neutrophils, the expression of CD200R was notably greater in neutrophils from CLP + ABX mice than in those from sham controls. (Fig. 1G). The surface expression of Ly6G increases as neutrophils mature [24], and here, we found that CD200R expression had an inverse relationship with Ly6G expression, further indicating an association with an immature phenotype (Fig. 1H). The observed changes in Ly6G and CD200R expression were not limited to bone marrow neutrophils but were also evident in circulating neutrophils (Fig. S3).

### Generation of $CD200R^{high}$ neutrophils is associated with impaired autophagy activation

Our finding that immature $CD200R^{high}$ neutrophils are generated by an immunosuppressive model led us to examine whether $CD200R^{high}$ neutrophils are different from their counterpart $CD200R^{low}$ neutrophils by comparing mRNA expression patterns after sorting the two populations, as shown in Fig. S4. RNA-seq analysis of the correlation matrix and multidimensional scaling indicated that $CD200R^{high}$ neutrophils were highly distinct from $CD200R^{low}$ neutrophils (Fig. 2A, B). Based on the ingenuity pathway analysis (IPA) analysis of the differentially expressed genes, $CD200R^{high}$ neutrophils were expected to have decreased activity in the autophagy pathway (Fig. 2C). Bulk RNA-seq revealed that $CD200R^{high}$ neutrophils had decreased expression levels of autophagy-related genes, including *Hif1a* and *Atg7* (Fig. 2D). Elongation and maturation of autophagosomes were expected to be attenuated in $CD200R^{high}$ neutrophils according to IPA (Fig. S5). Since autophagy in neutrophils is important for their maturation and proper function under inflammatory conditions [25], dysfunctional autophagy in $CD200R^{high}$ neutrophils correlates with a functionally immature neutrophil phenotype.

G-CSF is a granulopoietic cytokine that is primarily produced during inflammatory conditions [26]. It plays pivotal roles in both stimulating neutrophil production and enhancing the activities of various neutrophils, including ROS generation, phagocytosis, and cytokine production. G-CSF is also known for its ability to induce autophagy in neutrophils and hematopoietic stem cells [27]. We examined whether the autophagy status was reduced in $CD200R^{high}$ neutrophils from CLP + ABX mice using the autophagy-detecting agent CYTO-ID. Without any stimulation, there was no discernible difference between $CD200R^{high}$ and $CD200R^{low}$ neutrophils. However, when G-CSF was introduced, $CD200R^{high}$ neutrophils exhibited a decrease in $CYTO\text{-}ID^+$ cells (Fig. 2E). These results imply that $CD200R^{high}$ neutrophils exhibit impaired autophagy activation induced by G-CSF.

### $CD200R^{high}$ neutrophils are dysfunctional

$CD200R^{high}$ neutrophils exhibited an immature morphometric phenotype according to Giemsa staining (Fig. 3A). Since CD200R signaling limits inflammatory responses in myeloid cells [28] and autophagy activation is essential for neutrophil functions [29], we examined whether $CD200R^{high}$ and autophagy-impaired neutrophils are dysfunctional. Neutrophils are the first leukocytes recruited into an infected or injured area in diverse experimental disease models [30]. We thus compared the chemotactic migratory activities of two different neutrophil populations based on CD200R expression isolated from CLP + ABX mice. Compared with that in $CD200R^{low}$ neutrophils, chemotactic activity in $CD200R^{high}$ neutrophils was markedly decreased in response to several chemoattractants, such as CXCL2, MMK1, and fMLP (Fig. 3B). We then compared the expression of CXCR2 and CXCR4 by flow cytometry. Similarly, compared with that in $CD200R^{low}$ neutrophils, the expression of CXCR2 in $CD200R^{high}$ neutrophils was markedly decreased, while the level of CXCR4 was significantly increased (Fig. 3C). Transcriptome analysis of $CD200R^{high}$ neutrophils revealed that the levels of *Fpr1*, *Fpr2*, *Fpr3*, *Cxcr1* and *Cxcr2* were lower than those in $CD200R^{low}$ neutrophils (Fig. 3D), correlating with the different chemotactic activities of FPR family agonists and CXCL2, as shown in Fig. 3B.

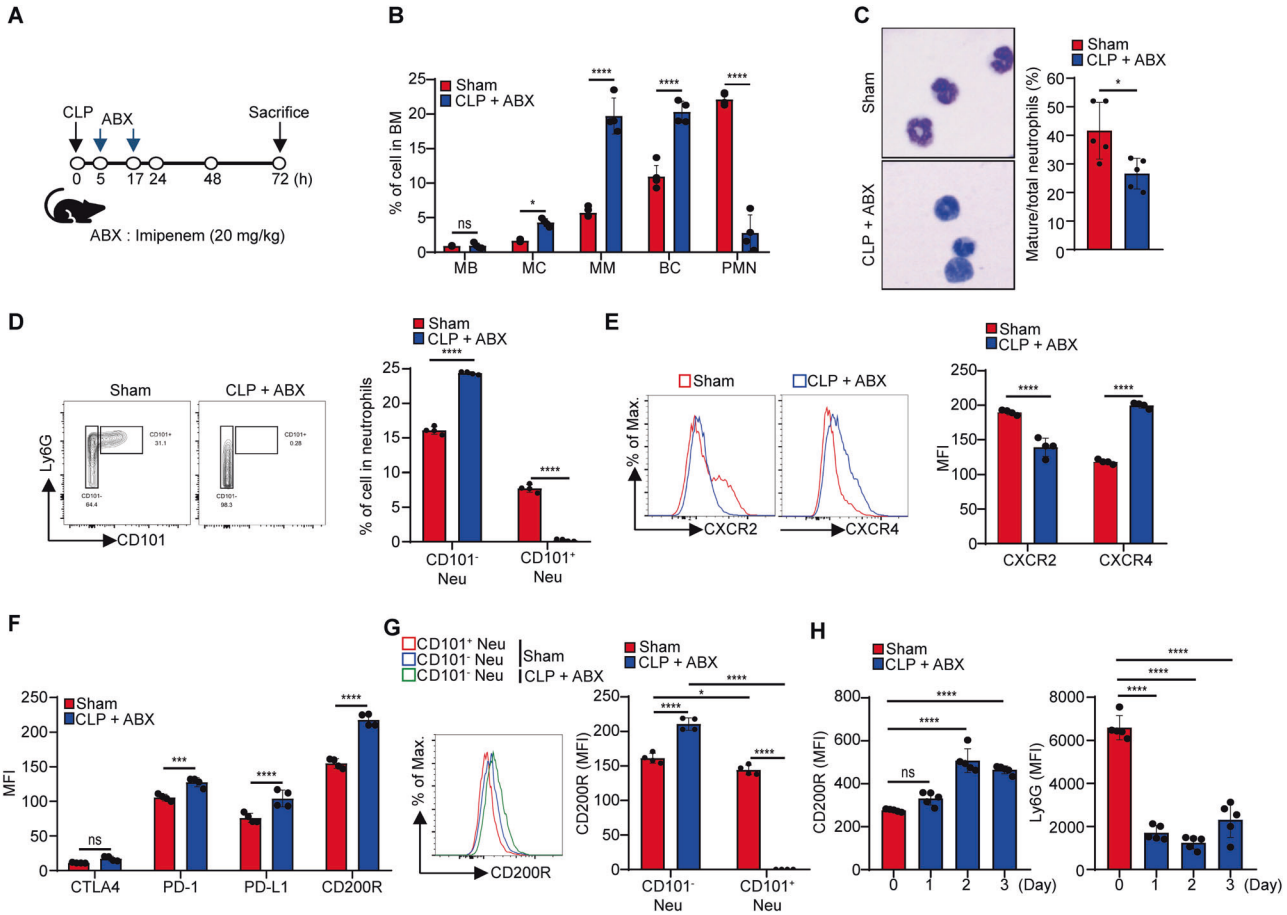


**Fig. 1** CD200R-expressing immature neutrophils were generated in vivo in an experimental sepsis-induced immunosuppressive model. **A**–**H** C57BL/6 mice were subjected to CLP surgery. ABX (imipenem, 20 mg/kg) was intraperitoneally injected two times into mice 5 h and 17 h after CLP. Treated mice were sacrificed 72 h after the surgery. **A** Model protocol for CLP + ABX mice. **B** Neutrophil development was assessed by measuring the expression of Ly6G and c-kit in both sham mice and CLP + ABX mice. [Ly6G$^-$ c-kit$^{high}$ myeloblasts (MBs), Ly6G$^-$ c-kit$^{mid}$ myelocytes (MCs), Ly6G$^{low}$c-kit$^{low}$ metamyelocytes (MMs), Ly6G$^{mid}$ c-kit$^{low}$ band cells (BCs), Ly6G$^{high}$c-kit$^{low}$ Polymorphonuclear neutrophils (PMNs)]. **C** Isolated bone marrow neutrophils from sham mice and CLP + ABX mice were stained with Giemsa staining solution, and mature neutrophils (segmented neutrophils) were counted under a light microscope. **D** Representative flow cytometry analysis of Ly6G and CD101 expression in neutrophils from sham and CLP + ABX mice. The bar graph indicates the percentage of CD101$^+$ and CD101$^-$ neutrophil subsets among total Ly6G$^+$ cells. **E** Representative flow cytometry histograms of CXCR2 and CXCR4 expression on neutrophils from sham and CLP + ABX mice. The bar graph indicates the quantified mean fluorescence intensity. **F** Surface expression of coinhibitory molecules (CTLA4, PD-1, PD-L1, and CD200R) on bone marrow neutrophils from sham mice and CLP + ABX mice was assessed by flow cytometry. **G** Representative flow cytometry histograms of CD200R expression on CD101$^-$ or CD101$^+$ neutrophils from sham or CLP + ABX mice. The bar graph indicates the quantified mean fluorescence intensity. **H** Sham and CLP + ABX mice were sacrificed at the indicated times, and neutrophil Ly6G and CD200R expression was assessed via flow cytometry. The data are representative of 4–5 mice per group from three independent experiments. The data are expressed as the mean ± SD. *$P < 0.05$; ***$P < 0.001$; ****$P < 0.0001$; ns not significant. Statistical significance was determined by Student's *t* test (**C**), one-way ANOVA (H), and two-way ANOVA (**B**, **D**, **E**–**G**)

A major function of neutrophils in innate defense is to kill invading microorganisms via superoxide anions [31]. Here, we tested superoxide anion production in response to PMA stimulation by the two different neutrophil populations. Although CD200R$^{low}$ neutrophils exhibited strong superoxide anion-producing activity, CD200R$^{high}$ neutrophils exhibited weak superoxide anion-producing activity (Fig. 3E). We also found that the expression of NADPH oxidase complex components (encoded by *Ncf1*, *Ncf2*, *Ncf4*, *Cyba*, and *Cybb*) was downregulated in CD200R$^{high}$ neutrophils compared to CD200R$^{low}$ neutrophils (Fig. 3F). LPS-stimulated cytokine production was also compared between the two neutrophil populations. LPS-stimulated production of TNF-α but not of IL-10 was significantly lower in CD200R$^{high}$ vs. CD200R$^{low}$ neutrophils (Fig. 3G). Collectively, these results suggest that, compared with CD200R$^{low}$ neutrophils, CD200R$^{high}$ neutrophils are dysfunctional with respect to chemotactic migration, superoxide anion production and TNF-α production.

## CD200 upregulation in an immunosuppressive model blocks autophagy in neutrophils

Since we found that the CLP + ABX model generates CD200R-expressing neutrophils (Fig. 1), we assessed the expression levels of the CD200R ligand CD200 in bone marrow cell types using the ImmGen database (http://rstats.immgen.org/Skyline/skyline.html). Interestingly, among the bone marrow cells, only B cells highly expressed *Cd200* mRNA (Fig. 4A). We found that the protein level of CD200 was also significantly increased on CD19$^+$ B cells from CLP + ABX mice (Fig. 4B). Previous studies reported that the membrane-bound form of CD200 undergoes cleavage, resulting in an increase in soluble CD200 (sCD200) in the circulation of tumor-induced immunosuppressive model mice [32, 33]. Although sCD200 is known to modulate macrophage function [28], whether sCD200 plays a functional role in neutrophils is unknown. We first found that sCD200 levels were increased in the bone marrow supernatants of mice with sepsis-induced immunosuppression

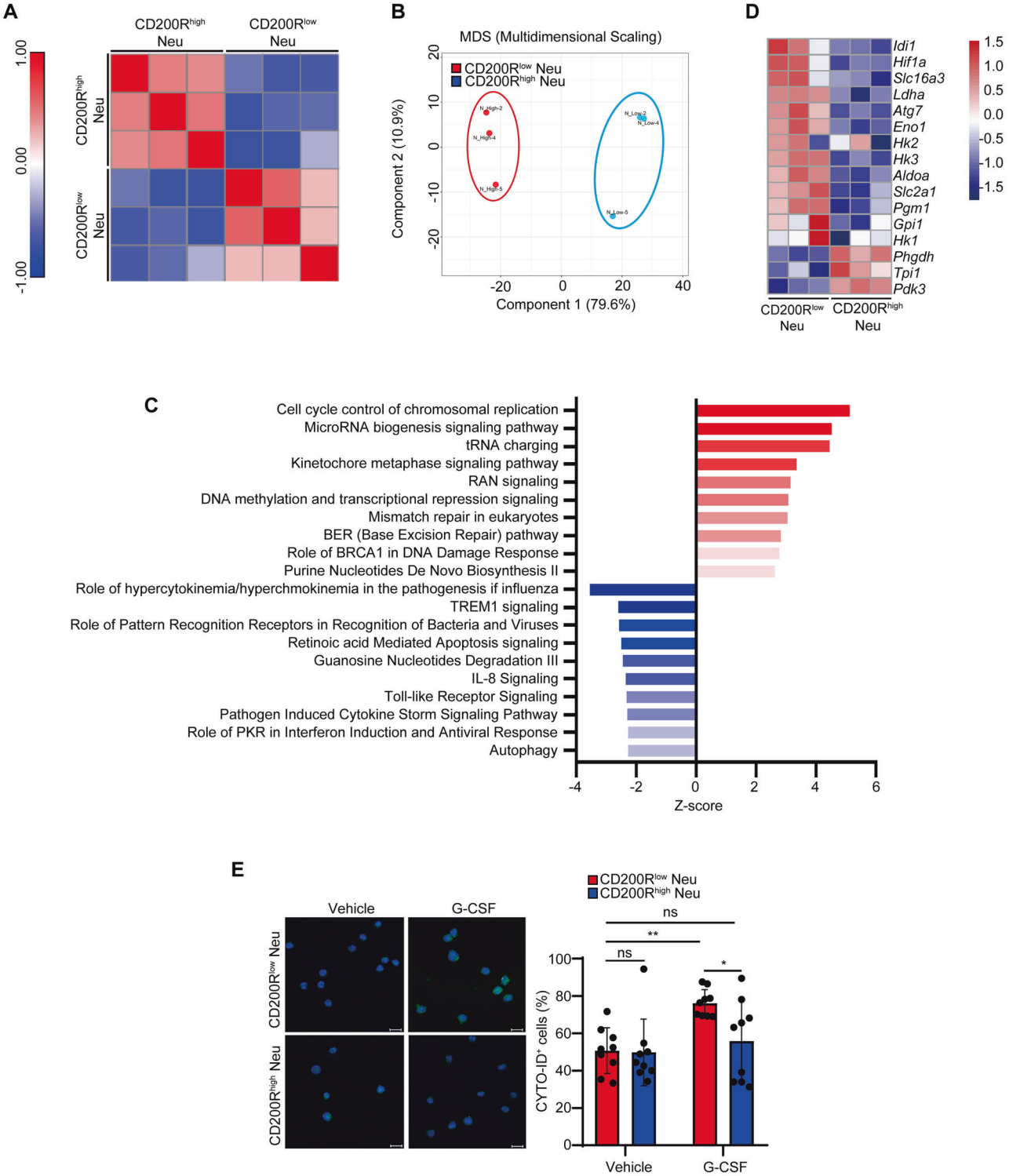


**Fig. 2** CD200R$^{high}$ neutrophils exhibit impaired autophagy. **A**–**E** C57BL/6 mice were subjected to CLP surgery. ABX (imipenem, 20 mg/kg) was intraperitoneally injected two times into mice 5 h and 17 h after CLP. The treated mice were sacrificed 72 h after surgery. Transcriptome analysis was also conducted on CD200R$^{low}$ and CD200R$^{high}$ neutrophils isolated from CLP + ABX mice. **A** Correlation matrix and **B** Multidimensional scaling was analyzed from bulk RNA-seq data of CD200R$^{low}$ neutrophils and CD200R$^{high}$ neutrophils. **C** Top 10 (red) and bottom 10 (blue) canonical pathways identified by ingenuity pathway analysis (IPA) in CD200R$^{high}$ neutrophils/CD200R$^{low}$ neutrophils. **D** Transcriptomic analysis of autophagy-related genes. The color of the symbols represents the upregulation (red) or downregulation (blue) of each gene according to the log2-fold change and $P \leq 0.05$ (**A**–**D**). **E** Isolated CD200R$^{low}$ and CD200R$^{high}$ neutrophils were treated with vehicle or G-CSF (100 ng/ml). CYTO-ID staining was carried out 6 h after G-CSF treatment, followed by analysis via confocal microscopy. A representative image is shown for CYTO-ID (in green) and Hoechst (in blue), with the scale bar indicating 10 μm. The data are expressed as the mean ± SD ($n = 9$ for **E**). *$P < 0.05$; **$P < 0.01$; ns not significant. Statistical significance was determined by two-way ANOVA (**E**)

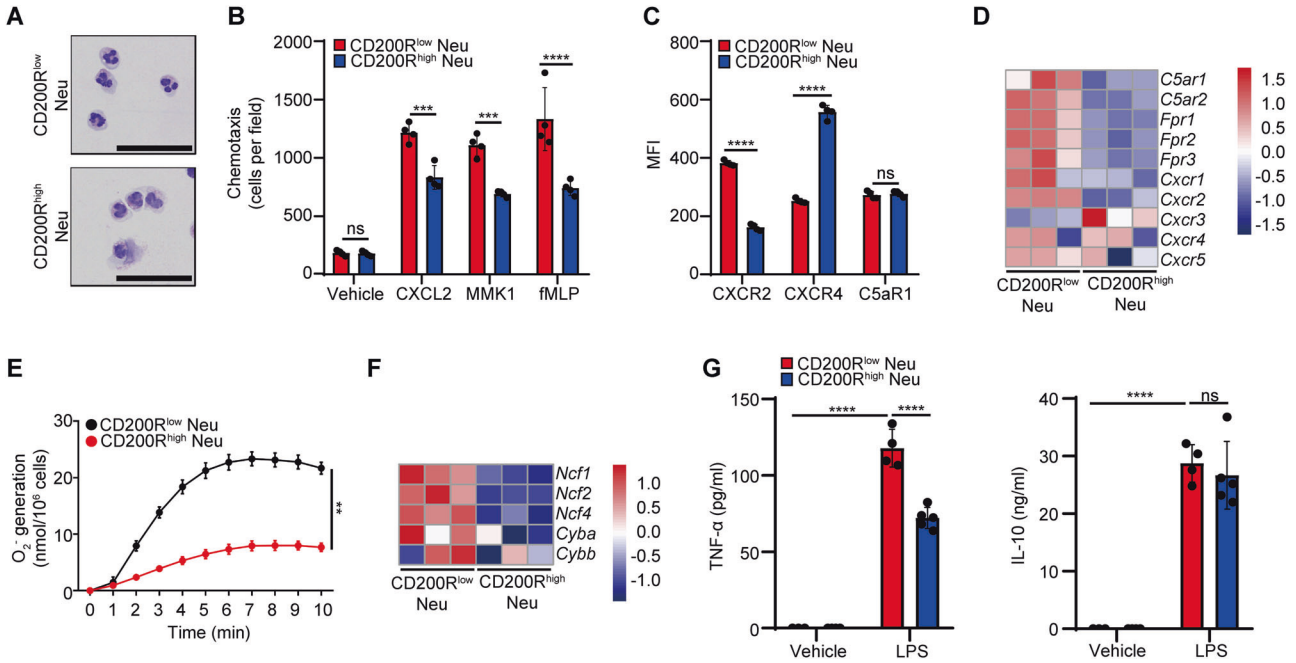


**Fig. 3** CD200R$^{high}$ neutrophils are dysfunctional. **A** Representative image of Giemsa-stained CD200R$^{high}$ and CD200R$^{low}$ bone marrow neutrophils isolated from CLP + ABX mice 72 h after surgery. **B** CD200R$^{high}$ and CD200R$^{low}$ neutrophils were assessed by chemotaxis assays using several stimuli (CXCL2, 30 ng/ml; MMK1, 1 μM; fMLP, 1 μM). **C** The surface expression of CXCR2 and CXCR4 on CD200R$^{high}$ and CD200R$^{low}$ neutrophils was measured by flow cytometry. **D** Gene expression of chemoattractant receptors (*C5ar1, C5ar2, Fpr1, Fpr2, Fpr3, Cxcr1, Cxcr2, Cxcr3, Cxcr4* and *Cxcr5*) was assessed via transcriptome analysis. **E** CD200R$^{high}$ and CD200R$^{low}$ neutrophils were stimulated with PMA (1 μM), and superoxide anion generation was measured using a cytochrome C reduction assay. **F** Transcriptome analysis of CD200R$^{high}$ and CD200R$^{low}$ neutrophils for the expression of *Ncf1, Ncf2, Ncf4, Cyba* and *Cybb*. **G** CD200R$^{high}$ and CD200R$^{low}$ neutrophils were stimulated with LPS (1 μg/ml) for 24 h. Cytokine levels were measured via ELISA. The data are representative of three independent experiments (**A**). The data are expressed as the mean ± SD ($n = 4$ for **B**, **C**, **E**; $n = 4$–5 for **G**). $^{**}P < 0.01$; $^{***}P < 0.001$; $^{****}P < 0.0001$; ns not significant. Statistical significance was determined by two-way ANOVA (**B**, **C**, **E**, **G**)

(Fig. 4C). *Cd200* mRNA levels in CD19$^+$ cells were not different between CLP + ABX mice and sham mice (Fig. 4D). The results indicated that both the membrane-bound and sCD200 levels were elevated in the CLP + ABX mice.

Next, we examined the effects of sCD200 on the neutrophil phenotype and activity using recombinant CD200 (rCD200; CD200-Fc) in the presence of G-CSF, a crucial factor for neutrophil maturation and one of the primary cytokines involved in sepsis [34]. During the maturation of bone marrow neutrophils induced by G-CSF, the addition of rCD200 blocked neutrophil maturation, resulting in elevated numbers of band cells compared to those in the vehicle control group (Fig. 4E left). Quantitative analysis revealed that rCD200 decreased the number of mature neutrophils in the presence of G-CSF (Fig. 4E right). We then examined the effects of rCD200 on autophagy in neutrophils. Stimulation of bone marrow neutrophils with G-CSF triggered autophagy, leading to increased numbers of CYTO-ID$^+$ cells, which were markedly attenuated by the addition of rCD200 (Fig. 4F). The inhibitory effect of rCD200 on neutrophil autophagy was abrogated by pretreatment with an α-CD200R antibody (Fig. S6). These findings suggested that an α-CD200R antibody can counteract the inhibitory impact of rCD200 in the presence of G-CSF in vitro. Functionally, bone marrow neutrophils incubated with rCD200 exhibited decreased chemotactic migration toward various chemoattractants, such as CXCL2, MMK1, and fMLP (Fig. 4G). rCD200 markedly reduced the secretion of TNF-α but not of IL-10 in response to LPS (Fig. 4H). These findings are consistent with the transcriptomic analysis, which revealed a decrease in the autophagic pathway in CD200R$^{high}$ neutrophils from CLP + ABX mice (Fig. 2), as well as with the observed impairment in the functional activities of CD200R$^{high}$ neutrophils (Fig. 3). Taken together, these results suggest that rCD200 may inhibit neutrophil maturation by blocking autophagy, leading to reduced functional activity.

### Administration of an α-CD200R antibody restores neutrophil maturation in CLP + ABX mice

To examine the functional roles of CD200R in neutrophils from CLP + ABX mice, we administered an α-CD200R antibody according to the protocol shown in Fig. 5A. Administration of the α-CD200R antibody effectively blocked surface CD200R expression on neutrophils (Fig. 5B). Surface Ly6G levels were significantly reduced in neutrophils from CLP + ABX mice compared with those from sham mice treated with a control IgG (Fig. 5C). Administration of the α-CD200R antibody significantly restored Ly6G expression on neutrophils in the CLP + ABX model (Fig. 5C). These results suggest that the administration of an α-CD200R antibody attenuates the inhibitory effects of CLP + ABX on neutrophil maturation. Since CLP + ABX inhibited autophagy activation and suppressed neutrophil maturation (Fig. 1) and CD200R$^{high}$ neutrophils exhibited decreased autophagy-related gene expression (Fig. 2), we examined the effects of the α-CD200R antibody on autophagy in neutrophils. Administration of the α-CD200R antibody to CLP + ABX mice enhanced autophagy activation, as evidenced by a notable increase in CYTO-ID$^+$ cells among neutrophils (Fig. 5D). Functionally, compared with neutrophils from control mice, neutrophils isolated from α-CD200R antibody-treated CLP + ABX mice exhibited increased superoxide anion production in response to PMA and *Staphylococcus aureus* (*S. aureus*) (Fig. 5E, F). These results suggest that the administration of the α-CD200R antibody inhibits the suppressive effects of CD200R on autophagy activity, restoring neutrophil maturation in vivo.

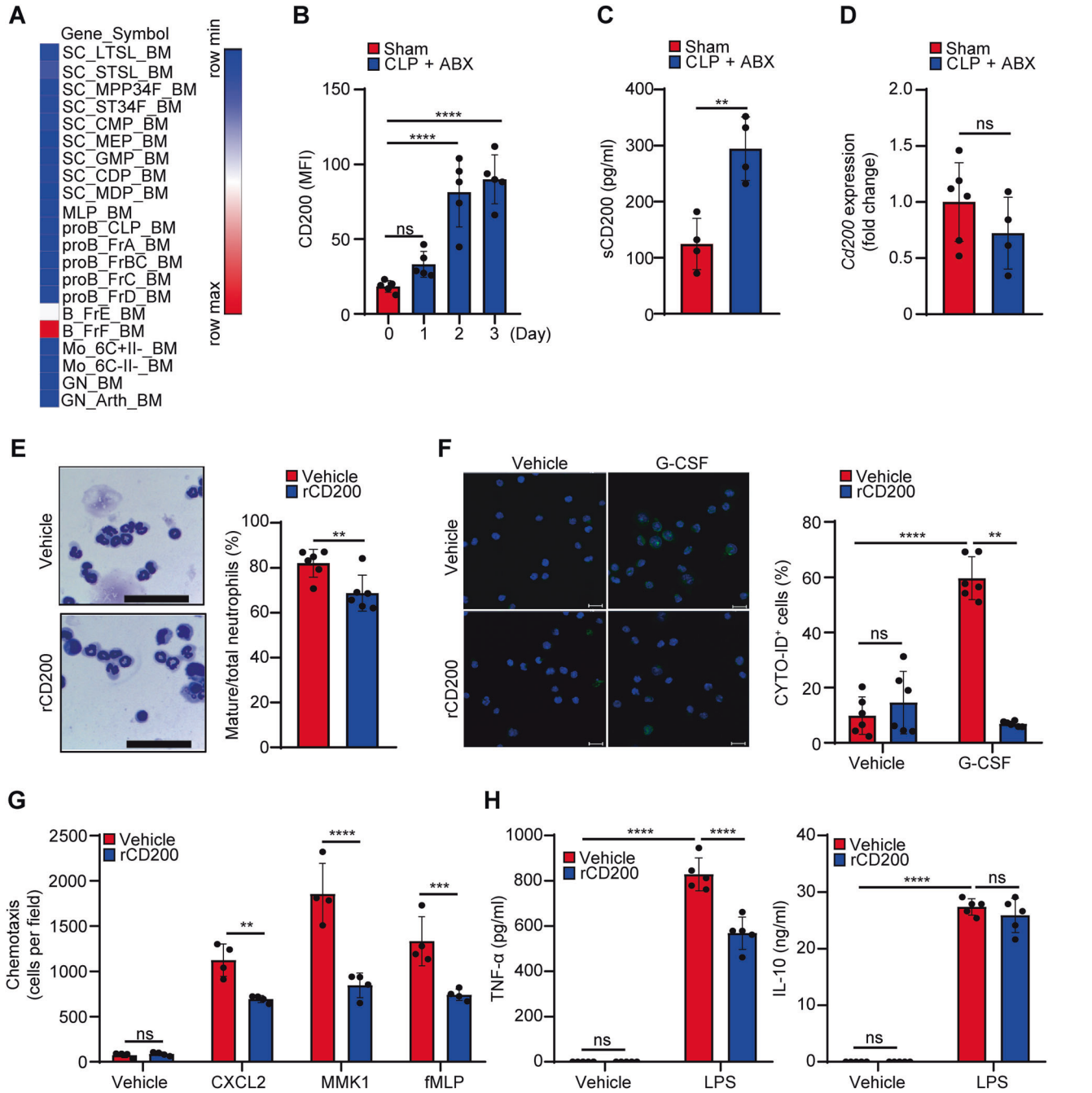


**Fig. 4** CD200 blocks neutrophil maturation by inhibiting autophagy. **A** The expression of CD200 in diverse cells found in the bone marrow from the ImmGen database. **B**–**D** C57BL/6 mice were subjected to CLP surgery. ABX (imipenem, 20 mg/kg) was injected intraperitoneally two times into mice 5 h and 17 h after CLP. Mice were sacrificed 72 h after surgery. **B** Surface expression of CD200 on $CD19^+$ bone marrow B cells from sham and CLP + ABX mice was measured via flow cytometry at the indicated time points. **C** sCD200 levels were measured in the cell-free lavage fluid of total bone marrow from sham and CLP + ABX mice. **D** *Cd200* mRNA expression was measured using qPCR in $CD19^+$ bone marrow B cells from sham and CLP + ABX mice 72 h after surgery. **E** Bone marrow neutrophils were preincubated with vehicle or rCD200 (2 μg/ml) for 6 h prior to the administration of G-CSF (100 ng/ml) and analyzed 12 h later. A representative image of Giemsa staining and the quantification of mature neutrophils were obtained by light microscopy (**E**). The scale bar represents 50 μm. **F** Bone marrow neutrophils were pretreated with vehicle or rCD200 (2 μg/ml) for 30 min before receiving G-CSF (100 ng/ml). CYTO-ID staining was conducted 6 h after G-CSF treatment, and the samples were subsequently analyzed via confocal microscopy. A representative image displaying CYTO-ID (in green) and Hoechst (in blue) is shown, with the scale bar indicating 10 μm. **G** The chemotaxis of vehicle- or rCD200-treated neutrophils toward several stimuli (CXCL2, 30 ng/ml; MMK1, 1 μM; fMLP, 1 μM) was assessed via chemotaxis assay. **H** Neutrophils were pretreated for 30 min with vehicle or rCD200 (2 μg/ml) and then incubated with or without LPS (1 μg/ml) for 24 h, after which the levels of TNF-α and IL-10 were measured via ELISA. The data are representative of at least three independent experiments. The data are expressed as the mean ± SD (n = 4–6). $^{**}P < 0.01$; $^{***}P < 0.001$; $^{****}P < 0.0001$; ns not significant. Statistical significance was determined by Student's *t* test (**C**–**E**), one-way ANOVA (**B**), and two-way ANOVA (**F**–**H**)

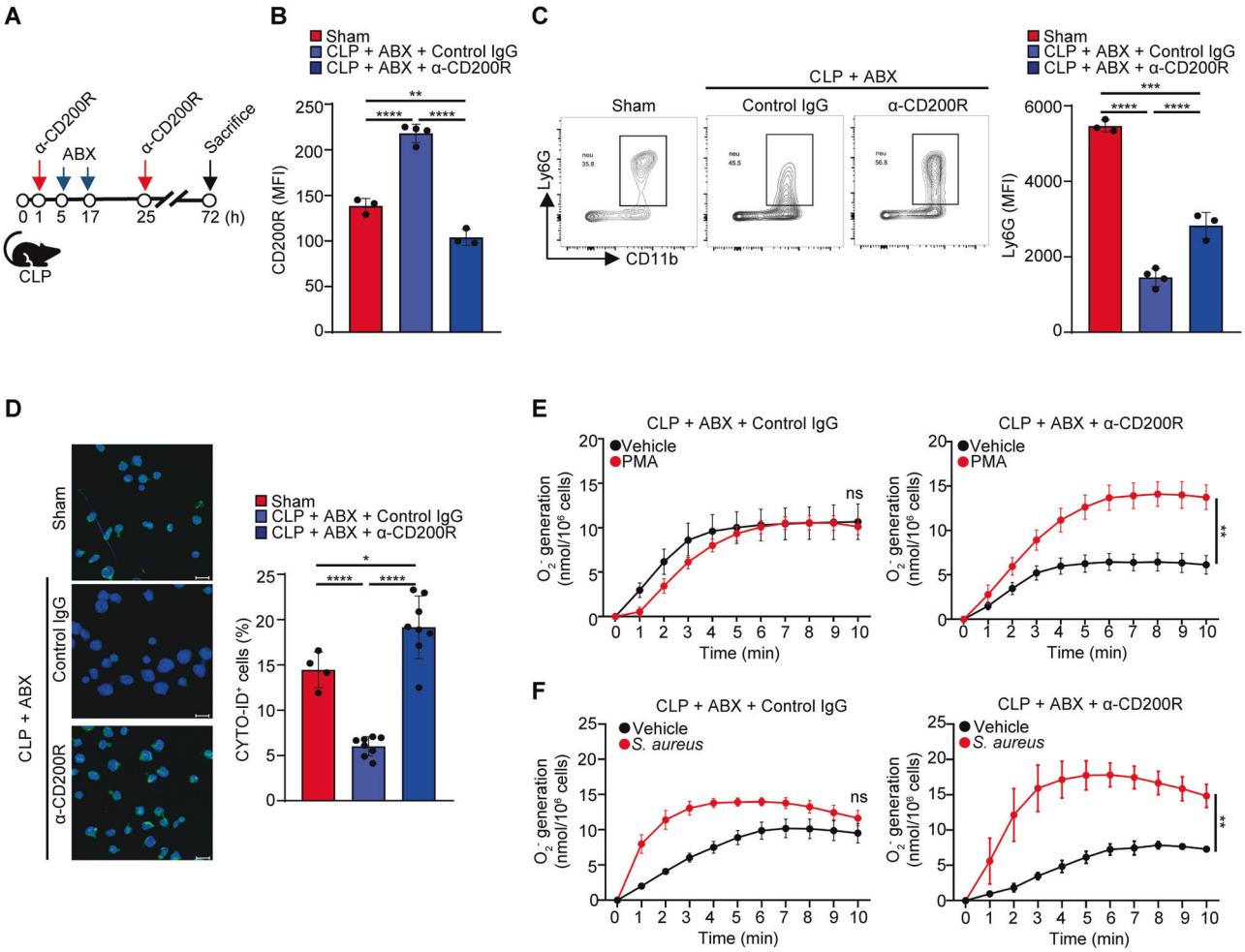


**Fig. 5** The administration of the α-CD200R antibody promoted the recovery of neutrophil maturation in CLP + ABX mice. **A** Model protocol for testing the effects of CD200R antibody treatment on neutrophil maturation. **B**–**F** C57BL/6 mice were subjected to CLP surgery. ABX (imipenem, 20 mg/kg) was injected intraperitoneally twice into mice 5 h and 17 h after CLP. An α-CD200R antibody (100 μg/mouse) or a control antibody (IgG2a, κ) was intraperitoneally injected two times into the mice 1 h and 25 h after CLP. Mice were sacrificed 72 h after surgery. Flow cytometric analysis of CD200R-expressing (**B**) and Ly6G-expressing (**C**) bone marrow neutrophils. **D**–**F** Bone marrow neutrophils were isolated from the mice. **D** Autophagic status was measured by CYTO-ID staining and analyzed by confocal microscopy. A representative image is shown for CYTO-ID (green) and Hoechst (blue), with the scale bar indicating 10 μm. **E** Superoxide anion production in response to PMA (1 μM) was measured by a cytochrome C reduction assay for 10 min. **F** Superoxide anion production was detected by a cytochrome C reduction assay in response to *S. aureus* ($1 \times 10^6$) for 10 min. The data are representative of three independent experiments. The data are expressed as the mean ± SD (n = 3–4 for **B**, **C**, **E**, **F**; $n = 4$, 8 for **D**). $^*P < 0.05$; $^{**}P < 0.01$; $^{***}P < 0.001$; $^{****}P < 0.0001$; ns not significant. Statistical significance was determined by one-way ANOVA (**B**–**D**) and two-way ANOVA (**E**, **F**)

### Administration of an α-CD200R antibody decreases mortality by suppressing immune cell apoptosis and lung inflammation in CLP + ABX mice challenged with secondary infection

We further evaluated the effects of the α-CD200R antibody in a secondary infection model with *S. aureus* following CLP + ABX, which mimics a clinical risk factor for mortality in septic patients, as shown in Fig. 6A. Administration of the α-CD200R antibody significantly increased the survival of CLP + ABX mice after secondary infection, as indicated by a 100% increase in survival compared to that in the control IgG group (50% survival) (Fig. 6B). Administration of the α-CD200R antibody to CLP + ABX mice also markedly suppressed lung inflammation (Fig. 6C left). The total number of cells in the airways was significantly decreased by α-CD200R antibody administration in the secondary infection model (Fig. 6C right). The production of several inflammatory cytokines, such as IL-1β, IL-6, and IL-10, was also decreased by α-CD200R antibody injection (Fig. 6D). The protective effect of the α-CD200R antibody was evident only in the context of secondary *S. aureus* infection following CLP + ABX but not in the case of primary *S. aureus* infection without CLP + ABX (Fig. S7). Leukocyte apoptosis is associated with increased mortality in experimental sepsis models [35, 36]. The establishment of the secondary infection model strongly increased splenocyte apoptosis, leading to a marked increase in TUNEL-positive cells in the spleen compared with that in the control IgG-injected group (Fig. 6E). However, administration of the α-CD200R antibody significantly decreased the number of TUNEL-positive cells in the spleen (Fig. 6E). We further examined which type of immune cell death was affected by α-CD200R antibody administration. The CLP + ABX secondary infection model mice exhibited markedly decreased numbers of $CD4^+$ T, $CD8^+$ T and $CD19^+$ B cells in the spleen, likely leading to immune suppression (Fig. 6F). However, α-CD200R antibody administration markedly increased the number of $CD19^+$ B cells and $CD8^+$ T cells but not the number of $CD4^+$ T cells (Fig. 6F). These results suggest that blocking CD200R in a secondary infection model specifically inhibits both B-cell and $CD8^+$ T-cell death, with a more pronounced effect on B-cell death.

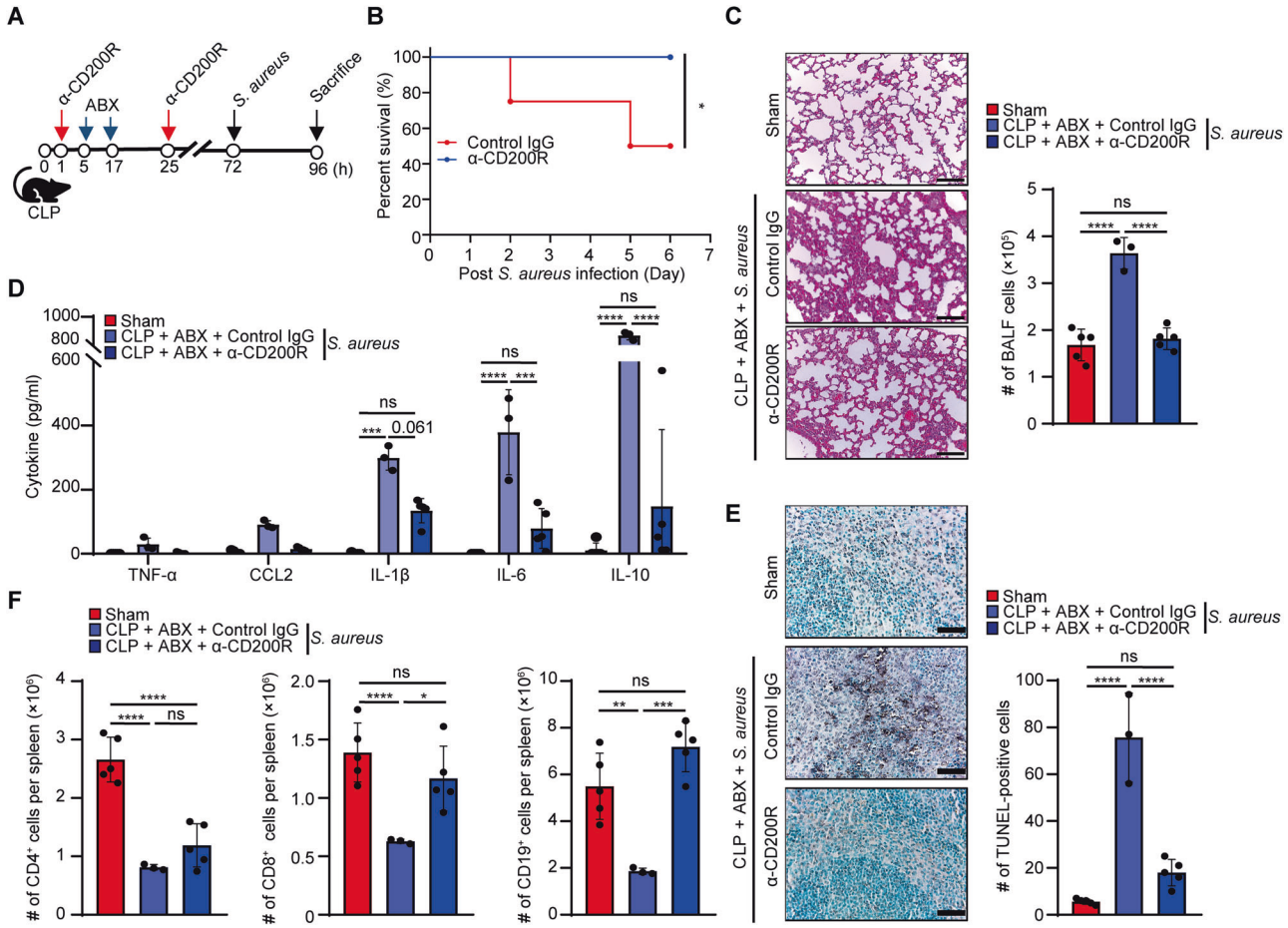


**Fig. 6** The administration of an α-CD200R antibody increases survival outcomes in CLP + ABX mice with secondary *S. aureus* infection. **A** Model protocol for testing the effects of α-CD200R antibody administration against a secondary infection in CLP + ABX mice. **B**–**F** C57BL/6 mice were subjected to CLP surgery. ABX (imipenem, 20 mg/kg) was intraperitoneally injected two times into mice 5 h and 17 h after CLP. The α-CD200R antibody (100 μg/mouse) was intraperitoneally injected two times into mice 1 h and 25 h after CLP. Mice were then infected with *S. aureus* ($1.5 \times 10^8$) 72 h after CLP. The survival rate was monitored for 6 days (**B**). **C**–**F** CLP + ABX mice were sacrificed 24 h after *S. aureus* infection. **C** Representative images of lungs stained with hematoxylin and eosin (scale bar = 100 μm), and the total number of cells in the BAL fluid was determined via a hemocytometer. **D** Cytokines, including TNF-α, CCL2, IL-1β, IL-6, and IL-10, were analyzed in the peritoneal fluid from sham mice, control IgG-injected mice and α-CD200R-injected mice. **E** A representative image of the TUNEL assay was performed on splenic tissue (scale bar = 100 μm), and the quantified number of TUNEL$^+$ cells is shown in the bar graph. **F** The numbers of splenic CD4$^+$ cells, CD8$^+$ cells and CD19$^+$ cells were measured via flow cytometry. The data are representative of three independent experiments. The data are expressed as the mean ± SD ($n = 3$–5 for **C**–**F**, and $n = 8$–10 for **B**). Statistical significance was determined by the log-rank test (**B**). * $P < 0.05$; ** $P < 0.01$; *** $P < 0.001$; **** $P < 0.0001$; ns not significant. Statistical significance was determined by one-way ANOVA (**C**, **E**, **F**) and two-way ANOVA (**D**)

### CD200R$^{high}$ neutrophil-derived IGF-1 increases $T_{reg}$ cells

Under sepsis-induced immunosuppression, a range of immunological phenotypes become apparent, encompassing not only the proliferation of dysfunctional immature neutrophils but also a decrease in lymphocyte numbers and increased T-cell exhaustion [37]. This diminished immune cell activity represents a substantial risk factor for both nosocomial infections and long-term immunological complications. To address this sepsis-induced immune cell dysfunction, clinical trials have been conducted to explore the targeting of immune checkpoint proteins by PD-L1- and CTLA4-specific antibodies [38]. We identified a novel population, CD200R$^{high}$ neutrophils, in an immunosuppressive animal model. Since CD200R is an immunomodulatory molecule, we investigated whether CD200R$^{high}$ neutrophils impact $T_{reg}$ cell numbers and activity. Through comparative transcriptome and qPCR analyses, we observed that bone marrow CD200R$^{high}$ neutrophils expressed higher levels of Igf1 than their CD200R$^{low}$ counterparts (Fig. 7A, B). In separate experiments, we found that splenic CD200R$^{high}$ neutrophils also expressed higher levels of Igf1 than CD200R$^{low}$ neutrophils (Fig. 7C). Both bone marrow CD200R$^{high}$ neutrophils and splenic CD200R$^{high}$ neutrophils expressed higher levels of the IGF-1 mRNA and protein than their CD200R$^{low}$ counterparts (Fig. 7B–D). Because IGF-1 is produced in the later stages of sepsis [39] and acts as an important inducer of $T_{reg}$ cells, which suppress immune responses [40], we asked whether neutrophils have an elevated capacity for IGF-1 production, which might contribute to immune suppression via $T_{reg}$ cell induction. Conditioned medium collected from the splenic neutrophils of CLP + ABX mice significantly increased the number of Foxp3$^+$ $T_{reg}$ cells in vitro (Fig. 7E). The effect of CD200R on the production of IGF-1 in the secondary infection model of CLP + ABX mice was examined, as depicted in Fig. 7F. Similarly, compared with those in the sham control mice, the levels of IGF-1 in the spleens of the secondary infection model mice were markedly increased; however, administration of the α-CD200R antibody significantly decreased IGF-1 levels, returning to sham control levels (Fig. 7G). We then investigated the role of CD200R in the generation of $T_{reg}$ cells in the secondary infection model. The

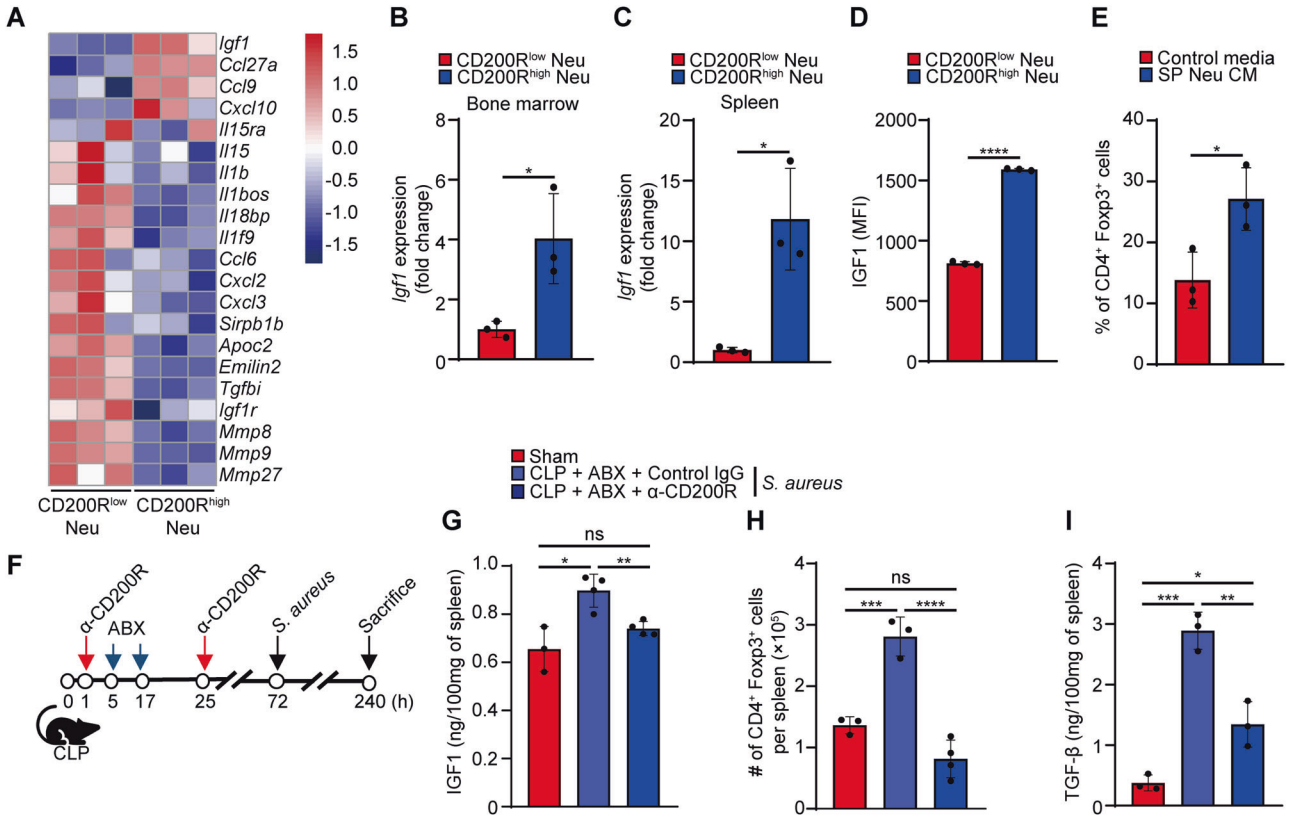


**Fig. 7** IGF-1 from CD200R$^{high}$ neutrophils induces $T_{reg}$ cell differentiation. **A** Transcriptome analysis of soluble factor genes from CD200R$^{high}$ and CD200R$^{low}$ neutrophils in the bone marrow. The gene expression of *Igf1* was measured by qPCR in CD200R$^{high}$ and CD200R$^{low}$ neutrophils from bone marrow (**B**) or the spleen (**C**). **D** The protein level of IGF-1 was measured by flow cytometry in CD200R$^{high}$ and CD200R$^{low}$ neutrophils from the spleen. **E** Flow cytometric analysis of CD4$^{+}$ Foxp3$^{+}$ cells was conducted after 72 h of differentiation. $T_{reg}$ cell differentiation was assessed with either control media or conditioned media from splenic neutrophils isolated 72 h after CLP + ABX challenge and cultured for 24 h. **F** Model protocol for testing the effects of α-CD200R antibody administration against secondary infection in CLP + ABX mice. **G–I** The mice were sacrificed on Day 7 post-*S. aureus* infection (1 × 10$^{8}$/mouse, intraperitoneal injection). **G** The level of IGF-1 in spleen homogenates was measured via ELISA. **H** The number of Foxp3$^{+}$ $T_{reg}$ cells was measured by flow cytometry. **I** The level of TGF-β in spleen homogenates was measured via ELISA. The data are representative of three independent experiments. The data are expressed as the mean ± SD ($n = 3$–4 for **B–E, G–I**). *$P < 0.05$; **$P < 0.01$; ***$P < 0.001$; ****$P < 0.0001$; ns not significant. Statistical significance was determined by Student's *t* test (**B–E**) and one-way ANOVA (**G–I**)

number of $T_{reg}$ cells in the spleen was substantially higher in the secondary infection model mice than in the sham control mice; however, the administration of the α-CD200R antibody significantly decreased the number of $T_{reg}$ cells (Fig. 7H). We also found that the level of TGF-β, a well-known cytokine produced by $T_{reg}$ cells, was strongly increased in the secondary infection model mice but was significantly decreased by α-CD200R antibody treatment (Fig. 7I). Thus, we hypothesize that the administration of an α-CD200R antibody can reverse the immunosuppressive effects of CD200R$^{high}$ neutrophils induced by CLP + ABX and further exacerbated by secondary bacterial infection with S. aureus by suppressing IGF-1-mediated $T_{reg}$ cell induction and TGF-β secretion.

## DISCUSSION

An important obstacle to developing effective sepsis treatments is the absence of experimental animal models that mimic the conditions of sepsis patients, particularly the confounding immunosuppression that occurs subsequent to sepsis onset. Over the years, researchers have developed more sophisticated and clinically relevant experimental sepsis-induced immunosuppression models, such as the CLP + ABX model. Although neutrophils are key innate immune cells that mediate host defense activity and are dysfunctional under septic conditions, their cellular and molecular dysfunctions have not been fully characterized. Here, we demonstrated that CD200R, an immune checkpoint receptor, is upregulated in immature neutrophils generated in mice challenged with CLP + ABX. CD200R$^{high}$ neutrophils exhibit an immature phenotype that includes significantly decreased chemotactic migration, superoxide anion production, and TNF-α production in response to LPS. Other reports have demonstrated that another checkpoint protein receptor, PD-1, is upregulated in lymphocytes, monocytes and macrophages in CLP-induced experimental sepsis [19, 41, 42]. Upregulated PD-1 may be a marker of monocyte dysfunction during sepsis [42]. Our results suggest that CD200R is a defining surface marker of dysfunctional neutrophils generated by sepsis-induced immunosuppression.

Accumulating evidence has demonstrated that autophagy is essential in the regulation of leukocyte differentiation in lymphocytes, monocytes, and dendritic cells [43–45]. However, there are contradictory reports on the functional role of autophagy in neutrophil differentiation [20, 46]. Rozman and colleagues demonstrated that neutrophil lineage-specific depletion of *Atg5* led to neutrophilia in vivo, suggesting that autophagy is not essential and, in fact, may play a negative role during neutrophil differentiation [46]. However, Riffelmacher et al. reported that autophagy is critical for neutrophil differentiation in vivo by supplying free fatty acids as an energy source for differentiation [20]. In this study, we observed reduced autophagy

in CD200R$^{high}$ neutrophils from CLP + ABX mice, as indicated by decreased numbers of CYTO-ID$^{+}$ cells (Fig. 2E). This reduction in autophagy was associated with the expansion of immature neutrophils. Our results suggest that CLP + ABX upregulates CD200R on neutrophils, which can lead to autophagy inhibition. Transcriptional analysis of sorted CD200R$^{high}$ and CD200R$^{low}$ neutrophils revealed that CD200R$^{high}$ neutrophils are highly distinct from CD200R$^{low}$ neutrophils, especially in terms of autophagy-related gene expression (Fig. 2A–D). IPA further supported our notion that CD200R$^{high}$ neutrophils exhibit defective autophagy (Fig. S5). G-CSF is a cytokine produced during inflammatory conditions that promotes granulopoiesis and augments neutrophil functions [26]. It has been extensively employed to combat chemotherapy-induced neutropenia, yielding substantial benefits. However, clinical trials involving G-CSF treatment for airway inflammation or nosocomial infections have not shown positive outcomes [47]. In separate experiments, we observed an increase in sCD200 in the bone marrow of CLP + ABX mice. Moreover, rCD200 effectively blocked neutrophil maturation in response to G-CSF by suppressing autophagy in vitro (Fig. 4E, F). Although diverse extracellular stimuli, including ligands for Toll-like receptors, G-protein coupled receptors and nutrient starvation, induce autophagy in neutrophils [25], the molecules that inhibit autophagy and the associated neutrophil maturation have yet to be revealed. Based on our findings, we suggest that sCD200 is an important negative regulator of neutrophil autophagy. We found that the administration of an α-CD200R antibody effectively abrogated the impact of rCD200 on G-CSF-induced autophagy in vitro (Fig. S6). We also observed that Ly6G levels were restored in neutrophils from CLP + ABX mice treated with the anti-CD200R antibody (Fig. 5C), suggesting that blocking CD200R in neutrophils can restore neutrophil maturation. Administration of the α-CD200R antibody to CLP + ABX mice also enhanced autophagy activation in neutrophils (Fig. 5D), resulting in the recovery of functional activity and the generation of superoxide anions in response to PMA and *S. aureus* infection (Fig. 5E, F). Taken together, our results suggest that CLP + ABX dampens autophagy in neutrophils and that administration of an α-CD200R antibody abrogates inhibitory signaling, restoring autophagy and enhancing neutrophil maturation. Therefore, the limited efficacy of G-CSF in treating sepsis-induced immunosuppression could be attributed to interference with G-CSF signaling via the CD200:CD200R pathway.

In this study, we note several limitations associated with the use of the α-CD200R antibody clone OX110. First, despite its common use for CD200R detection, this α-CD200R antibody has cross-reactivity with another member of the CD200R family, CD200RLc [48]. While our experimental mouse strain, C57BL/6, expresses multiple CD200R isoforms, including CD200R1, CD200RLa, CD200RLb, and CD200RLc, the α-CD200R antibody exhibits reactivity exclusively with CD200R1 and CD200RLc [48]. A previous report, however, demonstrated the absence of CD200RLc expression on CD11b$^{+}$ cells, both with and without stimulation [48]. We also failed to detect mRNA transcripts corresponding to CD200RLc (CD200R2) in our RNA-seq dataset. We therefore concluded that the binding of α-CD200R (OX110) to neutrophils is specific for CD200R and that any low-level cross-reactive binding to CD200RLc would be negligible. Second, because the same anti-CD200R antibody (OX110) was used for in vivo blockade and later for detection of CD200R on neutrophils by flow cytometry, it is possible that the observed decrease in CD200R staining was due to either functional effects of the in vivo antibody treatment on CD200R expression (e.g., binding and/or signaling leading to internalization and/or downregulation of receptor expression) or simple competitive binding to the same site on CD200R. Indeed, the reported half-life of mIgG2a in serum is 6 to 8 days [49]; therefore, the antibody should have been present at the time the neutrophils were analyzed. In either case, the data in Fig. 5B confirm that anti-CD200R treatment significantly reduced the levels of neutrophil CD200R available to interact with endogenous ligands (e.g., sCD200) in vivo. Third, this α-CD200R antibody has been characterized as an agonistic inhibitory antibody against CD200R in several studies [48, 50]. However, it does not exhibit an agonistic effect on CD200 in melanoma [51]. Despite conflicting reports regarding the agonistic or antagonistic effects of α-CD200R, we identified an antagonistic effect of the α-CD200R antibody within the scope of our investigation, where the α-CD200R antibody partially restored the diminished autophagy induced by rCD200 in G-CSF-treated neutrophils (Fig. S6). We hypothesize that the discrepancies in results between agonistic and antagonistic effects observed in different studies may be attributed to differences in experimental and disease contexts. In summary, while the mechanism of action of the α-CD200R antibody has not been determined, our findings suggest that targeting CD200:CD200R signaling could reverse sepsis-induced immunosuppressive phenotypes in neutrophils.

In clinical scenarios, neutrophil dysfunction is a crucial factor that heightens vulnerability to secondary nosocomial infections. In this study, we investigated whether α-CD200R antibody treatment could enhance the function of neutrophils to more effectively combat *S. aureus* infections. The administration of the α-CD200R antibody in experimental sepsis model animals led to numerous beneficial effects. Treatment with the anti-CD200R antibody significantly increased the survival rate of mice in the CLP + ABX model after secondary bacterial infection challenge by attenuating lung inflammation, inflammatory cytokine production, and immune cell apoptosis, particularly B lymphocyte apoptosis (Fig. 6B–F). Based on these findings, we concluded that CD200R normally plays an inhibitory role in host defense activities during sepsis-induced immunosuppression. This finding aligns well with the observed dysfunctional innate immune activities displayed by CD200R$^{high}$ neutrophils. Thus, targeting CD200R or CD200R$^{high}$ neutrophils may help to prevent or ameliorate the immunosuppression associated with clinical sepsis. Indeed, others have reported that blocking PD-1 or PD-L1 expression improved survival outcomes during experimental sepsis by reversing lymphocyte and monocyte dysfunction [19, 41], further supporting our notion that targeting immune checkpoint receptors or their ligands might prove beneficial for septic patients.

Other notable aspects of sepsis-induced immunosuppression include lymphopenia and the transformation of lymphocytes into a suppressive phenotype. Reduced lymphocytic activity poses a substantial risk for both nosocomial infections and long-term immunological complications. The complex immune response to sepsis is associated with $T_{reg}$ cells, which play important roles in immune suppression [39]. Although neutrophil dysfunction has been regarded as a crucial feature in the pathological progression of sepsis, the role of neutrophils in the regulation of $T_{reg}$ cells is largely unknown. Here, we found that CD200R$^{high}$ neutrophils expressed higher levels of *Igf1* and secreted more IGF-1 than CD200R$^{low}$ neutrophils (Fig. 7A–D). IGF-1 plays various roles in tissue development and function and is produced by the liver or peripheral cells to fulfill its functions. In addition to its endocrinological role, IGF-1 is involved in tissue regeneration and $T_{reg}$ cell induction [40]. Considering our findings that (i) conditioned medium collected from splenic neutrophils from CLP + ABX mice stimulated Foxp3$^{+}$ $T_{reg}$ cell generation (Fig. 7E); (ii) treatment with the α-CD200R antibody decreased IGF-1 levels and $T_{reg}$ cell numbers in the spleen in secondary infection model mice (Fig. 7G, H); and (iii) previous reports highlight the functional promote role of IGF-1 in generating $T_{reg}$ cells [39], we suggest that increased levels of IGF-1 from CD200R$^{high}$ neutrophils likely contributed to $T_{reg}$ cell generation in the secondary infection model of sepsis. These results suggest a link in which dysfunction of innate immune neutrophils regulates adaptive immune responses by generating $T_{reg}$ cells and thereby contributes to the pathological progression of sepsis.

In conclusion, in this study, we demonstrated that CD200R, an immune checkpoint receptor, is significantly upregulated in neutrophils during sepsis-induced immunosuppression. $CD200R^{high}$ neutrophils express high levels of IGF-1, which can induce $T_{reg}$ cell generation. Administration of an α-CD200R antibody elicited beneficial effects by augmenting neutrophil maturation and inhibiting $T_{reg}$ cell generation. Our results suggest that $CD200R^{high}$ neutrophils represent an important therapeutic target for sepsis.

## MATERIALS AND METHODS

### Sepsis-induced immunosuppression model

Eight-week-old male C57BL/6 mice were purchased from Orient Bio. All experiments involving animals received the approval of the Institutional Review Committee for Animal Care and Use at Sungkyunkwan University. The polymicrobial CLP-induced sepsis model was generated as described previously [52]. Briefly, mice were anesthetized with isoflurane and the cecum was exposed via an abdominal midline incision. The cecum was ligated and punctured with a 23-gauge needle and the abdomen was sutured. ABX (imipenem, 20 mg/kg) was intraperitoneally injected two times into CLP mice 5 h and 17 h after CLP. In antibody-treated mice, α-CD200R (100 μg/mouse) or a control antibody (IgG2a, κ) was injected intraperitoneally twice, 1 h and 25 h after CLP.

### Isolation of mouse bone marrow and spleen neutrophils

The femur, tibia and spleen were separated from CLP + ABX mice 72 h after surgery. After the bone marrow cells were flushed with PBS, a single-cell suspension was generated. Splenocytes were obtained by mechanical dissociation through a 40 μm cell strainer (SPL Life Sciences). Neutrophils were isolated from bone marrow cells using a neutrophil isolation kit (Biolegend).

### Giemsa staining

Isolated neutrophils ($2 \times 10^4$) were collected on cytoslides using cytospin centrifugation. Giemsa staining was conducted as previously described [53]. The cells were fixed with methanol and stained using diluted Giemsa solution (Sigma–Aldrich). After the stained cells were rinsed in deionized water, the samples were observed under a light microscope (Leica DM750).

### Flow cytometry

All flow cytometric analyses included discrimination of live/dead cells using Fixable Viability Dye (FVD) eFluor™ 780 (Thermo Fisher Scientific). The FACS buffer was prepared in-house with 0.5% BSA (Sigma–Aldrich) in PBS. Bone marrow cells and splenocytes were collected from sham and CLP + ABX mice 72 h after surgery and processed. The collected cells were stained with anti-Ly6G, anti-CD11b, anti-c-kit, anti-CD101, anti-CXCR4, anti-PD-1, anti-PD-L1, anti-CTLA4, anti-CD3e, anti-CD4, anti-CD8, anti-Foxp3, anti-CD19, anti-rabbit IgG (Thermo Fisher Scientific), anti-C5aR1, anti-CXCR2, anti-CD200 (R&D Systems), anti-CD200R (Bio-Rad) and anti-IGF-1 (Thermo Fisher Scientific) antibodies. For surface marker staining, the cells were incubated with antibodies in FACS buffer for 30 min at 4 °C. For intracellular staining, the cells were fixed and permeabilized using the FIX & PERM™ Cell Permeabilization Kit (Thermo Fisher Scientific). The fixing and staining protocol was conducted following the manufacturer's instructions. The stained cells were analyzed using a BD FACSCanto II flow cytometer and FlowJo analytical software (BD Biosciences).

### Sorting of $CD200R^{high}$ and $CD200R^{low}$ neutrophils

The femur, tibia and spleen were harvested from the experimental mice and processed. To isolate neutrophils, single-cell suspensions were stained with anti-CD200R-FITC, anti-CD11b-PerCPcy5.5, and anti-Ly6G-APC antibodies. $CD11b^+Ly6G^+CD200R^{high}$ or $CD11b^+Ly6G^+CD200R^{low}$ neutrophils were isolated using a BD FACS Aria™ III Cell Sorter (BD Biosciences).

### Transcriptome analysis and IPA

The whole-transcriptome expression data from the $CD11b^+Ly6G^+CD200R^{high}$ and $CD11b^+Ly6G^+CD200R^{low}$ neutrophils were analyzed by Macrogen, Inc., as previously described [54]. The total RNA concentration was determined using Quant-IT RiboGreen (Thermo Fisher Scientific). Total RNA from $CD11b^+Ly6G^+CD200R^{high}$ or $CD11b^+Ly6G^+CD200R^{low}$ neutrophils was analyzed using TapeStation RNA ScreenTape (Agilent Technologies). Only high-quality RNA preparations with an RNA integrity number greater than 7.0 were used for RNA library construction. The libraries were independently prepared with 1 μg of total RNA from $CD11b^+Ly6G^+CD200R^{high}$ or $CD11b^+Ly6G^+CD200R^{low}$ neutrophils using the Illumina TruSeq Stranded mRNA Sample Prep Kit (Illumina, Inc.). The library preparation workflow started with the purification of poly-A-containing mRNA molecules using poly-T-attached magnetic beads. Following purification, the mRNA was fragmented into small pieces using divalent cations at an elevated temperature. The cleaved RNA fragments were subsequently converted into first-strand cDNA using SuperScript II reverse transcriptase (Thermo Fisher Scientific) and random primers. This was followed by the synthesis of second-strand cDNA using DNA polymerase I, RNase H, and dUTP. The resulting cDNA fragments underwent an end repair process, followed by the addition of a single 'A' base and the ligation of adapters. The products were subsequently purified and enriched via PCR to generate the final cDNA library. The libraries were quantified using KAPA Library Quantification kits for Illumina Sequencing platforms following the qPCR Quantification Protocol Guide (KAPA BIOSYSTEMS), and their quality was assessed using TapeStation D1000 ScreenTape (Agilent Technologies). The indexed libraries were subsequently subjected to sequencing on an Illumina NovaSeq platform (Illumina, Inc.), where paired-end sequencing (2 × 100 bp) was performed by Macrogen, Inc. Differentially expressed mRNAs with $P \le 0.05$ between $CD200R^{high}$ neutrophils and $CD200R^{low}$ neutrophils were identified using the DESeq2 program in R and IPA (Qiagen).

### CYTO-ID and confocal microscopy

Isolated neutrophils were subjected to staining using the CYTO-ID® Autophagy Detection Kit (Enzo Life Sciences). The cells were incubated with CYTO-ID® reagent (diluted 1:500) in RPMI 1640 supplemented with 3% FBS for 30 min at 37 °C. Subsequently, the cells were seeded at a concentration of $1 \times 10^6$ cells per well in 24-well plates (Thermo Fisher Scientific) with coverslips coated with poly-L-lysine (Sigma–Aldrich). The cells were then fixed using 4% paraformaldehyde (Sigma–Aldrich) in PBS for 30 min at room temperature. Nuclei were stained with Hoechst (diluted 1:2,000; Thermo Fisher Scientific). The cover glasses were mounted onto glass slides and visualized using a Zeiss LSM700 microscope (Zeiss). The acquired images were subsequently processed with Zen software (Zeiss).

### Chemotaxis assay

Chemotaxis assays were carried out as described previously [53]. Sorted $CD200R^{high}$ neutrophils and $CD200R^{low}$ neutrophils were added to Boyden chambers with polycarbonate filters (3 μm) (Neuro Probe, Inc.) and incubated at 37 °C for 90 min. Nonmigrated cells were discarded from the filter after rinsing with PBS. The migrated cells were counted by using a light microscope after hematoxylin staining.

### Measurement of superoxide anion production

Sorted $CD200R^{high}$ neutrophils and $CD200R^{low}$ neutrophils were suspended in 100 μl of RPMI 1640 medium and stimulated with PMA (1 μM) or *S. aureus* ($1 \times 10^6$) in the presence of cytochrome C (50 μM) and cytochalasin B (5 μM). Superoxide generation was measured by monitoring the changes in light absorption at 550 nm by using a 96-well plate ELISA reader for 10 min at intervals of 1 min (Bio-Tek instruments).

### Secondary infection with *S. aureus*

*S. aureus* was grown overnight in tryptic soy broth. Bacteria were centrifuged at 3000 rpm for 10 min, after which the cells were washed with PBS. Bacterial counts were measured with a spectrophotometer at OD600 nm. CLP + ABX model mice were injected intraperitoneally with $1.5 \times 10^8$ *S. aureus*/mouse (survival data) or $1.0 \times 10^8$ *S. aureus*/mouse (tissue histology and immune cell population) 72 h after CLP.

### ELISA

Peritoneal fluid was harvested from sham, CLP + ABX + control IgG or CLP + ABX + α-CD200R mice at 24 h after secondary infection. Cultured media were collected 24 h after LPS stimulation from $CD200R^{high}$ or $CD200R^{low}$ neutrophils. The levels of cytokines (TNF-α, IL-6, CCL2, IL-1β, and IFN-γ) were measured via ELISA (Thermo Fisher Scientific). Spleens were obtained from the sham or CLP + ABX + Control IgG or CLP + ABX + α-CD200R groups on Day 7 after secondary infection. For quantification of IGF-1, spleens were homogenized in PBS using a homogenizer. The cell-

free supernatant was diluted after centrifugation for the assays. IGF-1 levels were measured by a Mouse/Rat IGF-1/IGF-1 Quantikine ELISA Kit (R&D). Total bone marrow supernatants were collected after centrifugation of the bone marrow cells obtained by flushing the femurs and tibias of sham or CLP + ABX mice. sCD200 levels were measured using the Mouse CD200 ELISA Kit PicoKine (Boster).

### Quantitative real-time PCR

Sorted cells ($CD200R^{low}$ and $CD200R^{high}$ neutrophils and $CD19^+$ cells) were lysed using TRIzol to isolate RNA. cDNA was generated with Maxine RT PreMix (iNtRON). qPCR was performed using the Rotor-Gene Q from QIAGEN with 2X Real-Time PCR Master Mix (BioFACT). The following primers were used for qPCR: *Igf1*-forward, 5′-AAAGCAGCCCCGCTCTATCC-3′; *Igf1*-reverse, 5′-CTTCTGAGTCTTGGGCATGTCA-3′; *Cd200*-forward, 5′-GAAGGTCTCAGGAA-CAGCTTGC-3′; *Cd200*-reverse, 5′-GCAGTCGCAGAGCAAGTGATGT-3′; and *Gapdh*-forward, 5′-CCACCACCCTGTTGCTGTA-3′, *Gapdh*-reverse, 5′-AATGTGTCCGTCGTGGATCT-3′. The qPCR data were quantified as ΔCt values for the *Igf1* and *Cd200* genes by using the 2-ΔΔCt method proportional to the expression of *Gapdh* as an internal control.

### Lung histology and TUNEL assay

Control IgG- or α-CD200R antibody-injected secondary infection model mice were sacrificed 24 h after surgery. Lungs were fixed in neutral buffered formalin, embedded in paraffin, sectioned into 4 μm sections, and stained with hematoxylin and eosin for microscopic analysis. For the TUNEL assay, the sections were permeabilized with 100 mM sodium citrate at 70 °C for 30 min and incubated with normal goat serum at room temperature for 30 min for blocking. After washing, TUNEL staining was performed using an In Situ Cell Death Detection Kit (Sigma–Aldrich) according to the manufacturer's instructions.

### Lung bronchoalveolar lavage (BAL) cell collection and counting

Control IgG- or α-CD200R antibody-injected secondary infection model mice were sacrificed at 24 h after surgery. After the mice were sacrificed, BAL fluid was collected with 900 μl of PBS using a catheter in the tracheal cannula. After centrifuging the same amount of BAL fluid, the cells were resuspended in PBS. The total number of cells in BAL fluid was determined using a hemocytometer.

### Differentiation of $T_{reg}$ cells

Naïve $CD4^+$ T cells were isolated from the spleens of C57BL/6 mice using a MagniSort™ Mouse $CD4^+$ naïve T-cell enrichment kit (Thermo Fisher Scientific). Isolated naïve CD4 T cells ($2 \times 10^6$/ml) were resuspended in complete RPMI 1640 medium supplemented with 10% FBS, anti-anti (Thermo Fisher Scientific), and 50 μM β-mercaptoethanol (Sigma–Aldrich). $T_{reg}$ cell differentiation was induced with anti-CD3e (2 μg/ml), anti-CD28 (2 μg/ml) and TGF-β (5 ng/ml) for 72 h, either with or without the addition of 100 μl of splenic neutrophil-conditioned medium.

### Statistical analysis

The results were evaluated using GraphPad Prism software. Statistical analysis was performed using one-way analysis of variance followed by Student's t test, one-way ANOVA, or two-way ANOVA, as appropriate. Survival data analysis was carried out using the log-rank test. All of the results are expressed as the mean ± SD. A $p$ value < 0.05 was considered to indicate statistical significance.

## REFERENCES

1. Hotchkiss RS, Moldawer LL, Opal SM, Reinhart K, Turnbull IR, Vincent JL. Sepsis and septic shock. Nat Rev Dis Prim. 2016;2:16045. https://doi.org/10.1038/nrdp.2016.45.
2. Hotchkiss RS, Karl IE. The pathophysiology and treatment of sepsis. N Engl J Med. 2003;348:138–50. https://doi.org/10.1056/NEJMra021333.
3. Vincent JL, Sun Q, Dubois MJ. Clinical trials of immunomodulatory therapies in severe sepsis and septic shock. Clin Infect Dis. 2002;34:1084–93. https://doi.org/10.1086/339549.
4. Presneill JJ, Harris T, Stewart AG, Cade JF, Wilson JW. A randomized phase II trial of granulocyte-macrophage colony-stimulating factor therapy in severe sepsis with respiratory dysfunction. Am J Respir Crit Care Med. 2002;166:138–43. https://doi.org/10.1164/rccm.2009005.
5. Zeiher BG, Steingrub J, Laterre PF, Dmitrienko A, Fukiishi Y, Abraham E, et al. LY315920NA/S-5920, a selective inhibitor of group IIA secretory phospholipase A2, fails to improve clinical outcome for patients with severe sepsis. Crit Care Med. 2005;33:1741–8. https://doi.org/10.1097/01.ccm.0000171540.54520.69.
6. Guillon A, Preau S, Aboab J, Azabou E, Jung B, Silva S, et al. Preclinical septic shock research: why we need an animal ICU. Ann Intensive Care. 2019;9:66. https://doi.org/10.1186/s13613-019-0543-6.
7. Kumar A, Roberts D, Wood KE, Light B, Parrillo JE, Sharma S, et al. Duration of hypotension before initiation of effective antimicrobial therapy is the critical determinant of survival in human septic shock. Crit Care Med. 2006;34:1589–96. https://doi.org/10.1097/01.CCM.0000217961.75225.E9.
8. Liu VX, Fielding-Singh V, Greene JD, Baker JM, Iwashyna TJ, Bhattacharya J, et al. The timing of early antibiotics and hospital mortality in sepsis. Am J Respir Crit Care Med. 2017;196:856–63. https://doi.org/10.1164/rccm.201609-1848OC.
9. Hotchkiss RS, Monneret G, Payen D. Sepsis-induced immunosuppression: from cellular dysfunctions to immunotherapy. Nat Rev Immunol. 2013;13:862–74. https://doi.org/10.1038/nri3552.
10. Alves-Filho JC, Spiller F, Cunha FQ. Neutrophil paralysis in sepsis. Shock. 2010;34:15–21. https://doi.org/10.1097/SHK.0b013e3181e7e61b.
11. Patel JM, Sapey E, Parekh D, Scott A, Dosanjh D, Gao F, et al. Sepsis induces a dysregulated neutrophil phenotype that is associated with increased mortality. Mediators Inflamm. 2018;2018:4065362. https://doi.org/10.1155/2018/4065362.
12. Kwok AJ, Allcock A, Ferreira RC, Cano-Gamez E, Smee M, Burnham KL, et al. Neutrophils and emergency granulopoiesis drive immune suppression and an extreme response endotype during sepsis. Nat Immunol. 2023;24:767–79. https://doi.org/10.1038/s41590-023-01490-5.
13. Nathan C. Neutrophils and immunity: challenges and opportunities. Nat Rev Immunol. 2006;6:173–82. https://doi.org/10.1038/nri1785.
14. Shi T, Ma Y, Yu L, Jiang J, Shen S, Hou Y, et al. Cancer immunotherapy: a focus on the regulation of immune checkpoints. Int J Mol Sci. 2018;19:1389. https://doi.org/10.3390/ijms19051389.
15. He X, Xu C. Immune checkpoint signaling and cancer immunotherapy. Cell Res. 2020;30:660–69. https://doi.org/10.1038/s41422-020-0343-4.
16. McBride MA, Patil TK, Bohannon JK, Hernandez A, Sherwood ER, Patil NK. Immune checkpoints: novel therapeutic targets to attenuate sepsis-induced immunosuppression. Front Immunol. 2020;11:624272. https://doi.org/10.3389/fimmu.2020.624272.
17. Noh H, Hu J, Wang X, Xia X, Satelli A, Li S. Immune checkpoint regulator PD-L1 expression on tumor cells by contacting CD11b positive bone marrow derived stromal cells. Cell Commun Signal. 2015;13:14. https://doi.org/10.1186/s12964-015-0093-y.
18. Melichar B, Nash MA, Lenzi R, Platsoucas CD, Freedman RS. Expression of costimulatory molecules CD80 and CD86 and their receptors CD28, CTLA-4 on malignant ascites CD3+ tumour-infiltrating lymphocytes (TIL) from patients with ovarian and other types of peritoneal carcinomatosis. Clin Exp Immunol. 2000;119:19–27. https://doi.org/10.1046/j.1365-2249.2000.01105.x.
19. Zhang Y, Zhou Y, Lou J, Li J, Bo L, Zhu K, et al. PD-L1 blockade improves survival in experimental sepsis by inhibiting lymphocyte apoptosis and reversing monocyte dysfunction. Crit Care. 2010;14:R220. https://doi.org/10.1186/cc9354.
20. Riffelmacher T, Clarke A, Richter FC, Stranks A, Pandey S, Danielli S, et al. Autophagy-dependent generation of free fatty acids is critical for normal neutrophil differentiation. Immunity. 2017;47:466–80.e5. https://doi.org/10.1016/j.immuni.2017.08.005.
21. Evrard M, Kwok IWH, Chong SZ, Teng KWW, Becht E, Chen J, et al. Developmental analysis of bone marrow neutrophils reveals populations specialized in expansion, trafficking, and effector functions. Immunity. 2018;48:364–79.e8. https://doi.org/10.1016/j.immuni.2018.02.002.
22. Eash KJ, Greenbaum AM, Gopalan PK, Link DC. CXCR2 and CXCR4 antagonistically regulate neutrophil trafficking from murine bone marrow. J Clin Investig. 2010;120:2423–31. https://doi.org/10.1172/jci41649.
23. Sledzinska A, Menger L, Bergerhoff K, Peggs KS, Quezada SA. Negative immune checkpoints on T lymphocytes and their relevance to cancer immunotherapy. Mol Oncol. 2015;9:1936–65. https://doi.org/10.1016/j.molonc.2015.10.008.
24. Deniset JF, Surewaard BG, Lee WY, Kubes P. Splenic Ly6G(high) mature and Ly6G(int) immature neutrophils contribute to eradication of S. pneumoniae. J Exp Med. 2017;214:1333–50. https://doi.org/10.1084/jem.20161621.
25. Shrestha S, Lee JM, Hong CW. Autophagy in neutrophils. Korean J Physiol Pharmacol. 2020;24:1–10. https://doi.org/10.4196/kjpp.2020.24.1.1.
26. Martin KR, Wong HL, Witko-Sarsat V, Wicks IP. G-CSF - a double edge sword in neutrophil mediated immunity. Semin Immunol. 2021;54:101516 https://doi.org/10.1016/j.smim.2021.101516.
27. Leveque-El Mouttie L, Vu T, Lineburg KE, Kuns RD, Bagger FO, Teal BE, et al. Autophagy is required for stem cell mobilization by G-CSF. Blood. 2015;125:2933–6. https://doi.org/10.1182/blood-2014-03-562660.
28. Chen EY, Chu S, Gov L, Kim YK, Lodoen MB, Tenner AJ, et al. CD200 modulates macrophage cytokine secretion and phagocytosis in response to poly(lactic co-

glycolic acid) microparticles and films. J Mater Chem B. 2017;5:1574–84. https://doi.org/10.1039/C6TB02269C.
29. Bhattacharya A, Wei Q, Shin JN, Abdel Fattah E, Bonilla DL, Xiang Q, et al. Autophagy is required for neutrophil-mediated inflammation. Cell Rep. 2015;12:1731–9. https://doi.org/10.1016/j.celrep.2015.08.019.
30. Kolaczkowska E, Kubes P. Neutrophil recruitment and function in health and inflammation. Nat Rev Immunol. 2013;13:159–75. https://doi.org/10.1038/nri3399.
31. Phan QT, Sipka T, Gonzalez C, Levraud JP, Lutfalla G, Nguyen-Chi M. Neutrophils use superoxide to control bacterial infection at a distance. PLoS Pathog. 2018;14:e1007157. https://doi.org/10.1371/journal.ppat.1007157.
32. Twito T, Chen Z, Khatri I, Wong K, Spaner D, Gorczynski R. Ectodomain shedding of CD200 from the B-CLL cell surface is regulated by ADAM28 expression. Leuk Res. 2013;37:816–21. https://doi.org/10.1016/j.leukres.2013.04.014.
33. Morgan HJ, Rees E, Lanfredini S, Powell KA, Gore J, Gibbs A, et al. CD200 ectodomain shedding into the tumor microenvironment leads to NK cell dysfunction and apoptosis. J Clin Invest. 2022;132:e150750. https://doi.org/10.1172/JCI150750.
34. Chousterman BG, Arnaud M. Is there a role for hematopoietic growth factors during sepsis? Front Immunol. 2018;9:1015. https://doi.org/10.3389/fimmu.2018.01015.
35. Schwulst SJ, Muenzer JT, Peck-Palmer OM, Chang KC, Davis CG, McDonough JS, et al. Bim siRNA decreases lymphocyte apoptosis and improves survival in sepsis. Shock. 2008;30:127–34. https://doi.org/10.1097/shk.0b013e318162cf17.
36. Luan YY, Yao YM, Xiao XZ, Sheng ZY. Insights into the apoptotic death of immune cells in sepsis. J Interferon Cytokine Res. 2015;35:17–22. https://doi.org/10.1089/jir.2014.0069.
37. Liu D, Huang SY, Sun JH, Zhang HC, Cai QL, Gao C, et al. Sepsis-induced immunosuppression: mechanisms, diagnosis and current treatment options. Mil Med Res. 2022;9:56. https://doi.org/10.1186/s40779-022-00422-y.
38. Chang KC, Burnham CA, Compton SM, Rasche DP, Mazuski RJ, McDonough JS, et al. Blockade of the negative co-stimulatory molecules PD-1 and CTLA-4 improves survival in primary and secondary fungal sepsis. Crit Care. 2013;17:R85 https://doi.org/10.1186/cc12711.
39. Nascimento DC, Melo PH, Pineros AR, Ferreira RG, Colon DF, Donate PB, et al. IL-33 contributes to sepsis-induced long-term immunosuppression by expanding the regulatory T cell population. Nat Commun. 2017;8:14919. https://doi.org/10.1038/ncomms14919.
40. Johannesson B, Sattler S, Semenova E, Pastore S, Kennedy-Lydon TM, Sampson RD, et al. Insulin-like growth factor-1 induces regulatory T cell-mediated suppression of allergic contact dermatitis in mice. Dis Model Mech. 2014;7:977–85. https://doi.org/10.1242/dmm.015362.
41. Brahmamdam P, Inoue S, Unsinger J, Chang KC, McDunn JE, Hotchkiss RS. Delayed administration of anti-PD-1 antibody reverses immune dysfunction and improves survival during sepsis. J Leukoc Biol. 2010;88:233–40. https://doi.org/10.1189/jlb.0110037.
42. Huang X, Venet F, Wang YL, Lepape A, Yuan Z, Chen Y, et al. PD-1 expression by macrophages plays a pathologic role in altering microbial clearance and the innate inflammatory response to sepsis. Proc Natl Acad Sci USA. 2009;106:6303–8. https://doi.org/10.1073/pnas.0809422106.
43. Miller BC, Zhao Z, Stephenson LM, Cadwell K, Pua HH, Lee HK, et al. The autophagy gene ATG5 plays an essential role in B lymphocyte development. Autophagy. 2008;4:309–14. https://doi.org/10.4161/auto.5474.
44. Zhang Y, Morgan MJ, Chen K, Choksi S, Liu ZG. Induction of autophagy is essential for monocyte-macrophage differentiation. Blood. 2012;119:2895–905. https://doi.org/10.1182/blood-2011-08-372383.
45. Lee HK, Mattei LM, Steinberg BE, Alberts P, Lee YH, Chervonsky A, et al. In vivo requirement for Atg5 in antigen presentation by dendritic cells. Immunity. 2010;32:227–39. https://doi.org/10.1016/j.immuni.2009.12.006.
46. Rozman S, Yousefi S, Oberson K, Kaufmann T, Benarafa C, Simon HU. The generation of neutrophils in the bone marrow is controlled by autophagy. Cell Death Differ. 2015;22:445–56. https://doi.org/10.1038/cdd.2014.169.
47. Bo L, Wang F, Zhu J, Li J, Deng X. Granulocyte-colony stimulating factor (G-CSF) and granulocyte-macrophage colony stimulating factor (GM-CSF) for sepsis: a meta-analysis. Crit Care. 2011;15:R58. https://doi.org/10.1186/cc10031.
48. Akkaya M, Aknin ML, Akkaya B, Barclay AN. Dissection of agonistic and blocking effects of CD200 receptor antibodies. PLoS ONE. 2013;8:e63325. https://doi.org/10.1371/journal.pone.0063325.
49. Vieira P, Rajewsky K. The half-lives of serum immunoglobulins in adult mice. Eur J Immunol. 1988;18:313–6. https://doi.org/10.1002/eji.1830180221.
50. Talebian F, Liu JQ, Liu Z, Khattabi M, He Y, Ganju R, et al. Melanoma cell expression of CD200 inhibits tumor formation and lung metastasis via inhibition of myeloid cell functions. PLoS ONE. 2012;7:e31442. https://doi.org/10.1371/journal.pone.0031442.
51. Pilch Z, Tonecka K, Skorzynski M, Sas Z, Braniewska A, Kryczka T, et al. The protumor effect of CD200 expression is not mimicked by agonistic CD200R antibodies. PLoS ONE. 2019;14:e0210796. https://doi.org/10.1371/journal.pone.0210796.
52. Lee SK, Kim SD, Kook M, Lee HY, Ghim J, Choi Y, et al. Phospholipase D2 drives mortality in sepsis by inhibiting neutrophil extracellular trap formation and down-regulating CXCR2. J Exp Med. 2015;212:1381–90. https://doi.org/10.1084/jem.20141813.
53. Park MY, Kim HS, Lee HY, Zabel BA, Bae YS. Novel CD11b(+)Gr-1(+)Sca-1(+) myeloid cells drive mortality in bacterial infection. Sci Adv. 2020;6:eaax8820. https://doi.org/10.1126/sciadv.aax8820.
54. Bae GH, Kim YS, Park JY, Lee M, Lee SK, Kim JC, et al. Unique characteristics of lung-resident neutrophils are maintained by PGE2/PKA/Tgm2-mediated signaling. Blood. 2022;140:889–99. https://doi.org/10.1182/blood.2021014283.

## ACKNOWLEDGEMENTS

This work was supported by Basic Science Research Program (NRF-2020M3A9D3038435, NRF-2017R1A5A1014560) and the Korea Initiative for Fostering the University of Research and Innovation Program (NRF-2020M3H1A1077095) through the National Research Foundation of Korea (NRF) funded by the Ministry of Science, ICT and Future Planning and by a grant from the Korea Health Technology R&D Project through the Korea Health Industry Development Institute (KHIDI), funded by the Ministry of Health & Welfare, Republic of Korea (grant number: HI22C2004).

## AUTHOR CONTRIBUTIONS

Y.K. designed and performed the research, analyzed the data, and wrote the paper. Y.J. designed and performed the research, analyzed data, and wrote the paper. G.B. designed the experiments and analyzed the data. J.K. performed the research and analyzed the data. M.L. designed the experiments and analyzed the data. B.A.Z. wrote the paper. Y.B. designed the research and wrote the paper.

## COMPETING INTERESTS

YSK, YSJ, and YSB have filed a patent related to this work. The other authors declare no competing interests.

## ADDITIONAL INFORMATION

**Supplementary information** The online version contains supplementary material available at https://doi.org/10.1038/s41423-024-01136-y.

**Correspondence** and requests for materials should be addressed to Yoe-Sik Bae.